

AttacKG: Constructing Technique Knowledge Graph from Cyber Threat Intelligence Reports

Zhenyuan Li
Zhejiang University

Jun Zeng
National University of Singapore

Yan Chen
Northwestern University

Zhenkai Liang
National University of Singapore

Abstract

Cyber attacks are becoming more sophisticated and diverse, making detection increasingly challenging. To combat these attacks, security practitioners actively summarize and exchange their knowledge about attacks across organizations in the form of cyber threat intelligence (CTI) reports. However, as CTI reports written in natural language texts are not structured for automatic analysis, the report usage requires tedious efforts of manual cyber intelligence recovery. Additionally, individual reports typically cover only a limited aspect of attack patterns (techniques) and thus are insufficient to provide a comprehensive view of attacks with multiple variants.

To take advantage of threat intelligence delivered by CTI reports, we propose AttacKG to automatically extract structured attack behavior graphs from CTI reports and identify the adopted attack techniques. We then aggregate cyber intelligence across reports to collect different aspects of techniques and enhance attack behavior graphs as technique knowledge graphs (TKGs). Such TKGs with technique-level intelligence directly benefit downstream security tasks that rely on technique specifications, e.g., Advanced Persistent Threat (APT) detection.

In our evaluation against 1,515 real-world CTI reports from diverse intelligence sources, AttacKG effectively identifies 28,262 attack techniques with 8,393 unique Indicators of Compromises (IoCs). Further, to verify AttacKG’s accuracy in extracting threat intelligence, we run AttacKG on eight manually labeled CTI reports. Empirical results show that AttacKG accurately identifies attack-relevant entities, dependencies, and techniques with F1-scores of 0.895, 0.911, and 0.819, which significantly outperforms the state-of-the-art approaches like EXTRACTOR [43] and TTPDrill [30].

1 Introduction

Advanced cyber security attacks are growing rapidly. The trend of cyber attacks is to adopt increasingly sophisticated and diverse tactics [10], such as multi-stage Advanced Persistent Threats (APTs), making detection more challenging

than ever before. To defend against the fast-evolving threat landscape, security practitioners actively gather and share knowledge about attacks on public resources, e.g., blogs and forums. Such cyber threat intelligence (CTI) is managed and exchanged typically in the form of either structured and machine-digestible Indicators of Compromise (IoCs) or unstructured and natural language CTI reports.

Structured threat intelligence defines cyber attacks using IoCs, which are artifacts in forensic intrusions, such as MD5 hashes of malware samples and IP/domains of command-and-control (C&C) servers. As IoCs can be easily adopted by cyber defense tools (e.g., intrusion detection systems), they have been widely utilized in security operation centers with open standards such as OpenIOC [9], STIX [6], and Cybox [3]. However, recent studies have shown that detection with disconnected IoCs is easy to bypass [34, 39]. For example, attackers can frequently change domains used in malware to evade detection. In comparison, by considering interactions among IoCs, graph-based detection typically demonstrates better robustness [26, 46] as it captures attack behaviors aligned to adversarial goals that are more difficult to be changed. Such IoC interactions can be found in unstructured CTI reports written by security practitioners based on their observations of attack scenarios in the wild. In particular, a well-written report will precisely describe attack behaviors through enumerating attack-relevant entities (e.g., CVE-2017-11882) and their dependencies (e.g., stager connecting to C&C sever).

CTI report provides a valuable source for understanding APT attacks [25, 28, 39, 40], where attackers prolong their presence on the target system by avoiding actions that arouse immediate suspicion before initiating devastating attacks. In particular, one canonical enterprise solution to detect APTs is to monitor system execution with audit logs and match logs against a knowledge base of security policies associated with known attack patterns, e.g., APT kill chains. Such specification-based detection typically relies on expert knowledge from existing CTI reports to reconstruct attack scenarios [40]. However, recovering attack behaviors from textual CTI requires non-trivial manual efforts. Intuitively, a system

capable of automatically extracting attack patterns from CTI reports can significantly benefit developing cyber defenses by reducing human efforts and speeding up response time. However, we identify two main challenges in expert knowledge extraction from CTI reports: (1) As CTI reports are written in an informal format, in natural languages, extracting structured attack behaviors needs to analyze semantics in unstructured CTI texts; (2) Attack knowledge is dispersed across multiple reports. Individual reports only focus on limited/incomplete attack cases, making it difficult to obtain a comprehensive view of attacks.

A commonly used structured representation of attack behaviors is the provenance graph [19, 31]. It forms the foundation for different security solutions, such as forensics investigation and abnormal behavior detection. Provenance graphs are typically constructed from low-level audit logs. By recognizing attack techniques in the provenance graph, analysts can also extract high-level summaries of multi-stage APTs, accelerating the investigation process. It is challenging to extract precise provenance-graph-based representation from the threat intelligence available in CTI reports. Our goal is to build an abstracted attack behavior graph (attack graph for short) to first explore interactions among system entities (e.g., files and processes) used in CTI reports. Further, we identify techniques in the attack graph based on general “Technique Templates” that aggregates technique knowledge from MITRE ATT&CK [11] in a graph structure. While prior studies [24, 36, 43] have attempted to automatically retrieve information from CTI reports, existing CTI parsing systems are not general enough. More specifically, existing parsers primarily focus on IoC-related behaviors while extracting attack behavior graphs. However, non-IoC entities are also semantic elements in the report that are critical for technique identification. For example, “email” in most cases indicate the `Phishing` technique in a CTI report.

In this paper, we propose `AttacKG` to aggregate threat intelligence across CTI reports for each technique and construct a knowledge-enhanced attack graph summarizing the technique-level attack workflow in CTI reports. Based on enhanced knowledge, we introduce a new concept which we call “Technique Knowledge Graph” (TKG) that summarizes causal techniques from attack graphs to describe the complete attack chain in CTI reports. We first adopt an attack graph extraction pipeline to parse a CTI report and extract attack-relevant entities and entity dependencies as an attack graph. Then, we initialize the technique templates using attack graphs built upon technique procedure examples crawled from MITRE ATT&CK knowledge base [11]. Next, we utilize a revised graph alignment algorithm to match technique templates in attack graphs. To this end, we can accurately align and refine the entities in both CTI reports and technique templates. While technique templates aggregate specific and probably new intelligence from real-world attack scenarios provided by CTI reports, attack graphs can utilize such knowledge in

templates to construct technique knowledge graphs (TKG).

We implement `AttacKG` and evaluate it against 7,373 examples of 179 techniques crawled from MITRE ATT&CK and 1,515 CTI reports collected from multiple intelligence sources, such as Cisco Talos Intelligence Group [1], Microsoft Security Intelligence Center [14], and DARPA Transparent Computing (TC) program [4]. Our experimental result demonstrates that `AttacKG` substantially outperforms existing CTI parsing solutions such as `EXTRACTOR` [43] and `TTPDrill` [30]: (1) with the CTI report parsing pipeline, `AttacKG` accurately constructs attack graphs from reports with F1-scores of 0.895 and 0.911 for entities and dependencies extraction, respectively; (2) based on extracted attack graphs, `AttacKG` accurately identifies adversarial techniques in the attack graph with an F1-score of 0.819; (3) `AttacKG` can successfully collect 28,262 techniques and 8,393 unique IoCs from 1,515 CTI reports.

In summary, we make the following contributions:

- We present `AttacKG`, an automated CTI report parser that can extract attack graphs from CTI reports and enrich graphs with aggregate cross-reports threat intelligence to form technique knowledge graphs (TKGs).
- We propose the design of the technique template to describe and collect general technique knowledge, and a revised graph alignment algorithm to identify attack techniques with templates. By aligning templates with the technique implementation in the attack graph, we exchange the knowledge from both to refine each other.
- We implement `AttacKG` and evaluate it with 1,515 real-world CTI reports. The result demonstrates that we can extract attack graphs from reports accurately and aggregate technique-level threat intelligence from massive unstructured CTI report accurately and effectively.

2 Background and Motivation

In this section, we first describe variants introduced by multi-stage cyber attacks, which pose additional challenges for detection. Then, we discuss how state-of-the-art detection approaches overcome such challenges and how the knowledge in CTI reports benefits them. Finally, we present a real-world CTI report as a motivating example for intuitive illustration.

2.1 Multi-stage Cyber Attacks and Variants

Cyber attacks nowadays are becoming more sophisticated and stealthy. A single cyber attack today typically consists of multiple stages with different attack techniques [25]. Especially, each technique accomplishes one or more tactical attack objectives. Attackers are quite flexible when generating such multi-stage attacks by taking alternative techniques or system entities (e.g., files and processes) to achieve the same adversarial goal. For example, both `T1547 - Boot or Logon Autostart Execution` and `T1053 - Scheduled`

The **threat actors** sent the trojanized Microsoft Word documents, probably via **email**. Talos discovered a **document** named *MinutesofMeeting-2May19.docx*. Once the victim opens the document, it fetches a remote template from the actor-controlled **website**, [http://droobox\[.\]online:80/luncher.doc](http://droobox[.]online:80/luncher.doc). Once the *luncher.doc* was downloaded, it used **CVE-2017-11882**, to execute **code** on the victim's machine. After the exploit, the file would write a series of base64-encoded **PowerShell commands** that acted as a **stager** and set up persistence by adding it to the *HKCU\Software\Microsoft\Windows\CurrentVersion\Run* Registry key.

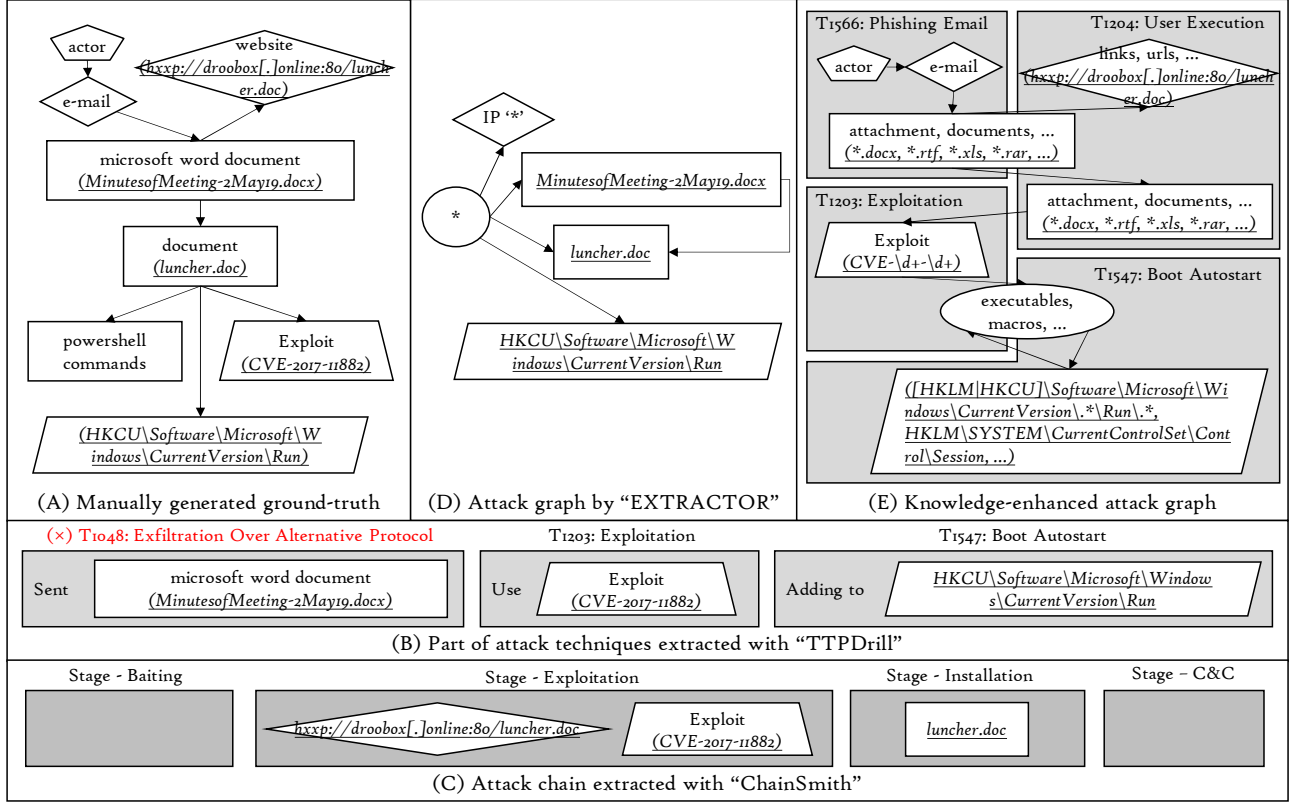


Figure 1: Motivating example - A comparison of different state-of-the-art CTI report parsers. The attack-relevant entities in the report sample are labeled with different colors according to their entity types, e.g., files. Underlined and italicized entities are IoCs, while the rest are non-IoC entities. In this graph, and the rest of the paper, we use boxes to denote files, diamonds to denote network connections, oval nodes to denote executables, pentagons denote attackers, trapezoidal nodes to denote vulnerabilities, and parallelogram nodes to denote registries and other system entities. Each edge represents a dependency between two entities. And (x) represents false positive techniques.

Table 1: An overview of tactics with the number of techniques, variants, IoCs (from MITRE and CTI reports).

Tactics	#Techs	#Variants	#IoCs from MITRE	#IoCs from reports
Reconnaissance	7	17	6	39
Resource Development	6	17	13	56
Initial Access	9	19	35	796
Execution	10	22	57	2025
Persistence	17	50	71	1423
Privilege Escalation	12	26	76	1312
Defense Evasion	32	70	126	2619
Credential Access	14	39	37	882
Discovery	22	50	96	2670
Lateral Movement	9	24	26	753
Collection	16	50	69	611
Command and Control	16	43	54	3333
Exfiltration	7	24	19	568
Impact	5	14	8	17
Total	182	465	693	17104

Task/Job can be used for persistence; in order to trick the victim into clicking while taking advantage of a "live-off-the-land" VBS execution environment, attackers can design attachments in either .doc or .xls format.

We automatically summarize such technique variants implemented with varying system entities and involved IoCs from technique examples provided by MITRE and massive real-world CTI reports. As Table 1 shows, we can extract 465 variants and 693 unique IoCs from 7,373 MITRE technique examples and 17,104 more unique IoCs from 1,515 CTI reports. That is to say, a typical cyber attack composed of three stages, namely, "Initial Access," "Privilege Escalation," and "Exfiltration" could roughly have $19 \times 50 \times 7 = 6650$ variations and involve $796 + 1312 + 568 = 1976$ unique IoCs. Details about how these variants and IoCs are extracted will be discussed in Section 3.3.3.

Therefore, detecting cyber attacks with the entire attack be-

havior as a signature is unreliable, which intuitively explains why emerging detection solutions try to detect independent attack techniques before further correlation analysis. This paper presents the first automatic approaches to aggregate technique-level threat intelligence from massive CTI reports, which can significantly improve the efficiency and coverage of attack detection.

2.2 Threat Detection with Provenance Graphs and Tactic-Technique-Procedure

Provenance graphs have been widely adopted for cyber threat detection and investigation for its powerful semantic expression ability and attack historic correlation ability [18, 25, 26, 29, 35, 39, 40, 46].

Typically, a provenance graph is composed of a set of system entities (e.g., processes, files, and networks) and interactions among entities (e.g., open, execute, and connect). Besides, provenance graphs will record the timestamps of interaction occurrence to support spatial and temporal analysis. With provenance graphs, security analysts can correlate malicious entities and abstract attack behaviors by causality analysis, which tracks potential information flow among entities [29] and provides a complete picture of the attack rather than a few fragmented and disconnected entities.

Nevertheless, a provenance graph built upon low-level system logs overgrows in size, making efficient detection difficult. To detect and investigate cyber threats in a timely manner, many existing approaches [25, 40] narrow down the search space by abstracting attack techniques locally from provenance graphs and building a high-level “Tactical Provenance Graph” (TPG). In particular, the TPG representation provides compact visualization of multi-stage attacks, which effectively accelerates the attack investigation process. However, the patterns used for technique detection are manually crafted, limiting the detection’s scalability and responsiveness.

To address this issue, we aim to automatically extract technique-level attack graphs in this paper from CTI reports and aggregate across-report technique knowledge into a new representation called “Technique Knowledge Graph” (TKG), which effectively reduces the workload and speeds up the response time.

2.3 Motivating Example

Figure 1 presents a real-world APT attack campaign called Frankenstein [5]. The campaign name comes from the ability of threat actors to piece together different independent techniques. As shown, this campaign consists of four attack techniques, such as T1566 – Phishing E-mail and T1547 – Boot Autostart. Each technique involves multiple entities and dependencies to accomplish one or more tactical attack objectives.

It is a typical multi-stage attack campaign that nowadays consists of multiple atomic techniques. To evade detection, such attacks can be morphed easily by replacing any technique with an alternative one. Therefore, it is recommended to detect and investigate cyber attacks at the technical level [25, 30, 35, 39], which is more robust and semantically richer.

Research progress has been made to automatically extract knowledge about attacks from CTI reports. Subfigures (B) to (D) show the information retrieved from the report sample by EXTRACTOR [43] TTPDrill [30], and ChainSmith [49], respectively, while Subfigure (A) represents the manually generated ground-truth. Subfigure (D) presents the attack graph generated by EXTRACTOR with IoCs and dependencies. Note that EXTRACTOR aggregates all non-IoC entities of the same type and thus loses the structural information of attack behaviors, making it impossible to identify the technique accurately. Subfigure (B) shows attack techniques identified by TTPDrill with manual-defined threat ontology. As shown, TTPDrill can only extract separate techniques from CTI reports without the whole picture. Besides, the ontologies provided by TTPDrill containing only action-object pairs for technique identification are too vague to lead to many false positives. As the example shows, sending a document is recognized as exfiltration in TTPDrill. However, in this scenario, the “trojanized” document is sent by an attacker for exploitation. Detailed comparisons are demonstrated in Section 4. As shown in Subfigure (C), ChainSmith provides a semantic layer on top of IoCs that captures the role of IoCs in a malicious campaign. They only give a coarse-grained four-stage classification with limited information.

Subfigure (E) illustrates the ideal result we want to extract in this paper. As long as we can identify attack techniques in attack graphs extracted from CTI reports, we are able to enrich the attack graphs with more comprehensive knowledge about the corresponding techniques. For example, we can find more possible vulnerabilities that can be used in T1203 – Exploitation for Execution as a replacement for CVE-2017-11882 appeared in this report. Moreover, the distinct threat intelligence can be collected and aggregated at the technique level across massive reports.

3 Approach

3.1 Overview of AttackKG

Figure 2 shows the architecture of AttackKG. At a high level, AttackKG has two subsystems: (1) an attack graph extraction pipeline for CTI reports parsing and attack graphs building, and (2) an attack technique identification subsystem for technique template generation and technique identification in attack graphs. We provide a brief overview of the workflow of AttackKG below, with more implementation details discussed in Section 3.2 and 3.3, respectively.

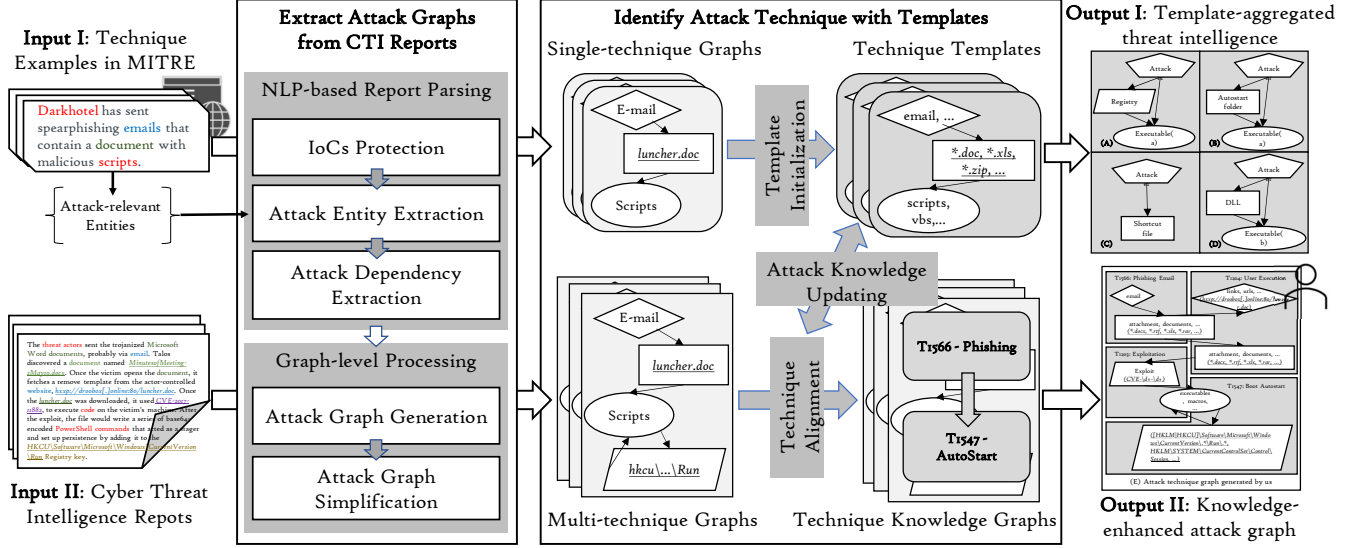


Figure 2: Overview of AttackKG architecture. AttackKG takes two inputs: (1) technique procedure examples from MITRE describing individual attack techniques; (2) real-world CTI reports describing end-to-end attack workflow, and provides two outputs: (1) technique templates that aggregate technique-level threat intelligence across reports; (2) attack graphs enhanced with aggregated technique intelligence. Details of Output I and II can be found in Figure 3 and 1, respectively.

Extract Attack Graphs from CTI Reports. To accurately extract attack graphs from CTI reports, we design a pipeline of five stages: (1) IoC protection, (2) Attack entities extraction, (3) Attack dependency extraction, (4) Attack graph generation, and (5) Attack graph simplification, as Figure 2 shows.

Specifically, we first extract attack-relevant entities from CTI reports with regular expressions and a customized NLP module. Then, we retrieve intra-sentence dependencies with NLP dependency parsing component and inter-sentence dependencies with resolved co-reference. Finally, we are able to generate the attack graph with entities as nodes and dependencies among them as edges.

As shown in Figure 2, this pipeline has two inputs: (1) technique procedure examples crawled from MITRE ATT&CK describing individual techniques, and (2) CTI reports describing multi-technique attack campaigns. These two inputs are isomorphic, and the corresponding outputs of the pipeline are (1) single-technique graphs and (2) multi-techniques graphs for attack campaigns.

Identify Attack Technique with Templates As discussed in Section 2, individual reports typically have a limited aspect of attack patterns without a global vision. In this paper, we aim to bridge this gap by aggregating threat intelligence across CTI reports with technique templates. Specifically, we propose technique templates to aggregate technique-level intelligence and a revised graph alignment algorithm to identify techniques in attack graphs to achieve this goal.

As Figure 2 shows, technique templates are initialized with single-technique attack graphs extracted from technique examples crawled from MITRE. Then we adopt the revised

attack graph alignment algorithm to identify attack techniques in multi-technique graphs extracted from real-world CTI reports with the pre-initialized templates. With the aligned nodes in the attack graph and the corresponding technique template, we can enhance the attack graph with general knowledge in templates as TKG and update the technique template with rich threat intelligence from CTI reports at the same time.

Finally, we obtain two outputs: (1) technique templates that collect and aggregate attack knowledge across massive CTI reports at the technique level; (2) Technique Knowledge Graphs (TKGs) summarizing the whole attack chains in CTI reports.

3.2 CTI Reports Parser

In this section, we discuss our primary approach for extracting attack graphs from CTI reports. Well-written CTI reports include detailed technical descriptions of how attack-related entities interact to accomplish specific objectives in attack campaigns. Despite the rich information, it is challenging to accurately extract attack behaviors from CTI reports written in natural language. Specifically, we identify four challenges:

- **C1. Domain-specific terms.** CTI reports often contain numerous security-related terms such as IoCs and attack family names. These domain-specific terms could include special characters, which confuse most off-the-shelf NLP modules.
- **C2. Non-IoC entities extraction.** Except for IoCs that can be easily extracted with regular expressions, there are many non-IoC entities in the form of varied natural

language descriptions, which also play critical roles in attack behaviors.

- **C3. Dependencies extraction.** As opposed to provenance graphs that record attack actions with full details, CTI reports are often written in a more summarized manner, just providing an overview of the attack workflow. Thus, the attack graphs extracted from CTI reports demonstrate coarse-grained and incomplete causal dependencies among entities rather than precise attack activities.
- **C4. Co-reference resolution.** Co-reference is very common in natural language. We identify two types of co-reference in CTI reports. Explicit co-references use pronouns like “*it*,” “*this*,” etc. or definite article “*the*”, while implicit co-references use synonyms to refer to entities that appear in the preceding text.

To the best of our knowledge, AttackG is the first CTI report parser to solve all four challenges simultaneously. In particular, **C1** are solved by IoC protection as described in Subsection 3.2.1; Subsection 3.2.2 and 3.2.3 tackle **C2** and **C3** with customized NLP models, respectively; **C4** is partly solved in Subsection 3.2.2 with co-reference resolution and the remainder is solved in Subsection 3.2.4 by graph simplification.

3.2.1 IoC Recognition and Protection with Regex

CTI reports contain numerous domain-specific terms, such as CVE-2017-21880 and /etc/passwd/, which includes special characters and thus confuses general NLP models. In order to avoid the influence of these terms while preserving the information of attack behaviors, we identify their types with a refined version of open-source IoC recognizer [7] and replace them with commonly used words according to their entity types. And we will record the location of replaced words for subsequent resumption of the IoCs.

After excluding domain-specific terms with special characters that affect the effectiveness of the NLP module, we are able to adopt standard models [15] for report parsing.

3.2.2 Attack Entity Extraction

In addition to IoCs entities, non-IoC entities also play important roles in attack technique expression. For better extraction, as shown in Table 2, we classify non-IoC entities into seven types. Among them, Actor and Executable represent subjects of attack behaviors, while File, Network connection, and Registry denote common system-level objects. Further, we identify several “other” types of entities that are difficult to directly map to system objects but frequently appear in certain techniques. We place them in a separate category.

Then, we adopt a learning-based Named Entity Recognition (NER) model to recognize entities in CTI reports. The

Table 2: Attack-relevant Entities (Both IoCs and non-IoCs)

Entity Types	Subject /Object	Entity Terms
Actor	Subject	apt, cobalt, rat, actor, lazarus, jrat, ...
Executable	Subject	command, malware, script, payload, vbs, ...
File	Object	files, directory, document, attachments, ...
Network	Object	c2, http, remote, email, server, host, links, ...
Registry	Object	registry, keys.
Vulnerability	Object	vulnerability, exploit.
Others	Object	service, credentials, account, wmi, task, ...

model is pre-trained on a large general corpus ¹ and re-trained with technique examples randomly selected from MITRE covering all techniques and entity types. In addition, to improve the accuracy of entity extraction, we use a customized rule-based entity recognizer ² to identify well-defined and common entities. We will record the type and location of identified entities for subsequent steps.

Finally, We adopt an open-source co-reference resolver, coreferee ³, for explicit co-references resolution. All pronouns for an attack-relevant entity are recorded in a linked table, and the corresponding nodes will be merged when constructing the attack graph.

3.2.3 Attack Dependency Extraction

Caused by the ambiguity of natural language, it is difficult to extract the exact dependency types between entities. For example, the same preposition *with* can represent completely different operations: (“*E-mail with malicious attachment*” meaning **downloading** a malicious attachment from a E-mail server while “*Document with macro*” meaning **executing** a macro script when opening a document. Therefore we will not take these uncertain dependency types to guarantee the generality of the attack graph.

Concretely, we first construct a dependency tree for each sentence with a learning-based nature language parsing model [15]. Then we enumerate all pairs of attack-relevant entities (including their pronouns) and estimate the distance between them with the distance of their Lowest Common Ancestor (LCA) and the distance of their position in the sentence. Each entity will establish dependencies with its nearest entity unless there is only one entity in the sentence.

3.2.4 Attack Graph Generation and Simplification

Given attack entities and dependencies in CTI reports, we model an attack behavior as a graph with nodes representing attack-relevant entities and edges representing dependencies, which we call *attack technique graph* (G_a) in this paper.

¹https://github.com/explosion/spacy-models/releases/tag/en_core_web_sm-3.1.0

²<https://spacy.io/api/entityruler>

³<https://github.com/msg-systems/coreferee>

So far, we have only considered the dependencies between entities within sentences. To establish cross-sentence dependencies and remove redundant nodes, we need to merge both explicit and implicit co-reference nodes. (C3) General NLP models can recognize explicit co-reference. And we will identify implicit co-references based on entities' type and character-level overlap.

Finally, we generate a concise and clear attack graph describing all attack behaviors that appear in a CTI report. Our evaluations on a wide range of CTI reports demonstrate that AttackKG attack graph extraction pipeline is accurate (Section 4.2.1) and effective (Section 4.2.3).

3.3 Technique Templates and Graph Alignment Algorithm

In order to identify specific techniques from the attack graph while accurately extracting the corresponding threat intelligence mentioned in the CTI report, we first need a universal description of attack technique. In this paper, we adopt a design of technique template with graph structure for each technique.

Then, inspired by the graph alignment algorithm used in Poirot [40] for attack behavior identification in provenance graph, we design a revised graph alignment algorithm for technique identification with templates. The algorithm has two main objectives: (1) Identify attack techniques involved in the attack graph with the similarity-based alignment score; (2) Determine what roles attack graph nodes play in the attack technique. Finally, we introduce how to initialize and update technique templates with alignment results on single-technique attack graphs.

3.3.1 Design of Technique Templates

To present the attack behaviors inside techniques while aggregating threat intelligence, we model technique templates also as graphs (G_t) with statistics information. In the graph, nodes represent aggregated entity knowledge, and edges represent possible dependencies among them.

An example of the technique template is demonstrated in Figure 3 and Table 3. As shown, a technique template typically involves multiple nodes and edges to accomplish an adversarial objective. Each node may have multiple different expressions in different reports, either with IoC terms or natural language descriptions. We will collect and store these expressions in IoC term set (i_{IoC}), NLP description set (i_{NLP}) for each node. Besides, technique descriptions in different reports may involve different combinations of entities for different variants and sometimes involve non-necessary entities. Thus, we record the occurrence number (i_{occur}) of entities across technique descriptions in different reports to measure their importance to the technique.

Similarly, for edges representing dependencies between entities, to illustrate the importance of each dependency, we record the occurrence number ($(i \dashrightarrow j)_{occur}$) for all the dependencies ($i \dashrightarrow j$).

3.3.2 Graph Alignment for Technique Identification and Technique Knowledge Graph Construction

We demonstrate our main approach for alignment between technique template G_t and attack graph G_a by defining the alignment score to measure how proper an alignment is. Specifically, as shown in Table 4, we define two kinds of alignments, i.e., node alignment between two nodes in two different graphs, and graph alignment measuring the overall similarity between a technique template and a certain sub-graph in the attack graph.

Node alignment. We first enumerate every node k in attack graph G_a to find node alignment candidates for every node i in a template G_t by calculating the alignment score for nodes $\Gamma(i : k)$. The alignment score between two nodes is computed by Equations (1) and (2):

$$\Gamma(i : k) = \begin{cases} \gamma + (1 - \gamma) \cdot \text{Sim}(i, k) & i_{type} = k_{type} \\ 0 & i_{type} \neq k_{type} \end{cases}, \quad (1)$$

$$\text{Sim}(i, k) = \text{Max}(\text{sim}(i_{IoC}, k_{IoC}), \text{sim}(i_{NLP}, k_{NLP})). \quad (2)$$

Intuitively, if node i and node k have different types, then the alignment score will be zero. Otherwise, they will get a basic type-matched score γ . Then the similarity of nodes' attributes ($\text{Sim}(i, k)$) can be determined by enumerating and calculating terms in the IoC term set and natural language description set similarity ($\text{Sim}(i, k)$) at the character level [8]. If the alignment score reaches a pre-defined threshold, we will record the node alignment candidates in a list for each corresponding template node.

Graph alignment. Afterward, we iterate through all candidate nodes to calculate the overall alignment scores $\Gamma(G_t :: G_a)$ in two parts: node-level alignment scores $\Gamma_N(G_t :: G_a)$ and edge-level alignment scores $\Gamma_D(G_t :: G_a)$. Specifically, the alignment score between a technique template and an attack graph can be computed by Equations (3), (4), and (5):

$$\Gamma_N(G_t :: G_a) = \sum_{i \in G_t, k \in G_a} (\Gamma(i : k) \cdot i_{occur}) / \sum_{i \in G_t} (i_{occur}), \quad (3)$$

$$\Gamma_D(G_t :: G_a) = \sum_{\substack{i \dashrightarrow j \in G_t \\ k \dashrightarrow l \in G_a}} \left(\frac{(\Gamma(i : k) \cdot \Gamma(j : l))}{C_{\min}(k \dashrightarrow l)} \cdot (i \dashrightarrow j)_{occur} \right) / \sum_{i \dashrightarrow j \in G_a} ((i \dashrightarrow j)_{occur}), \quad (4)$$

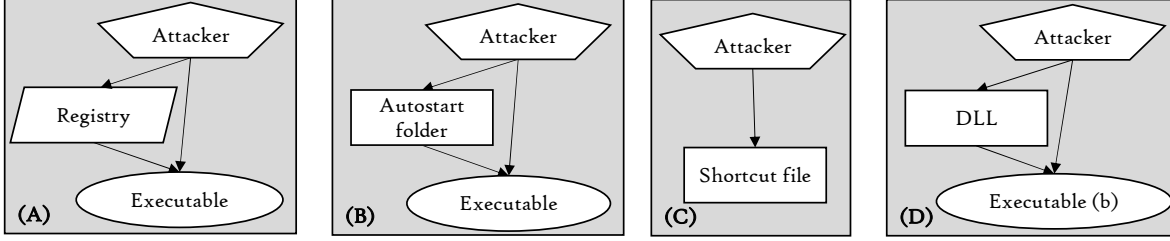


Figure 3: Technique template generated by AttackKG for T1547 - Boot or Logon Autostart Execution with four variants corresponding to fourteen MITRE sub-techniques categorized as (A) Registry Run Keys, (B) Auto-start folder, (C) Shortcut Modification, and (D) DLL Side-loading.

Template entity	Natural language descriptions	IoC terms
Executable	macros, scripts, malware, ...	*.exe, *.ps1, ...
Register	register, register keys, ...	HKLM/software/microsoft/windows/currentversion/[run/runonce/svchostload]/*, HKLM/system/currentcontrolset/control/print/*, HKLM/software/microsoft/windows/currentversion/winlogon/*, HKLM/software/microsoft/active setup/installed components/*, ...
Autostart folder	startup folder, path, ...	~/config/autostart/*, %Startup%*, %HOMEPATH%\Start Menu\Programs\Startup\, ...
Shortcut file	shortcut, ...	*.lnk, ...
DLL	malicious DLL, SSP DLL, winlogon helper DLL, ...	sspisrv.dll ...

Table 3: Attack Entities in the template of the technique T1547 - Boot or Logon Autostart Execution.

Table 4: Notations in Graph Alignment

Notation	Description
$i : k$	Node alignment between node i and k from different graph
$i \dashrightarrow j$	An dependency (path) from node i to node j
$G_t :: G_a$	Graph alignment between Template G_t and Graph G_a
$\Gamma(i : k)$	Alignment score between node i to node j
$\Gamma(G_t :: G_a)$	Alignment score between Template G_t and Graph G_a
$\Gamma_N(G_t :: G_a)$	Node-level alignment score between Template G_t and Attack Graph G_a
$\Gamma_D(G_t :: G_a)$	Dependency-level alignment score between Template G_t and Attack Graph G_a

$$\Gamma(G_t :: G_a) = \frac{1}{2} \cdot (\Gamma_N(G_t :: G_a) + \Gamma_D(G_t :: G_a)). \quad (5)$$

As shown, the node-level alignment score ($\Gamma_N(G_t :: G_a)$) is a weighted sum of the alignment score ($\Gamma(i : k)$) of each node. The weights are proportional to the number of node occurrences (i_{occur}) recorded in the template. While the dependency-level alignment score ($\Gamma_D(G_t :: G_a)$) depends on the alignment scores of the nodes at both ends of the dependency ($\Gamma(i : k)$ and $\Gamma(j : l)$), the minimal hop between both ends of the dependency ($C_{min}(k \dashrightarrow l)$) in the attack graph, and the number of node occurrences ($((i \dashrightarrow j)_{occur})$) recorded in the template. If the nodes at the end of the dependency are not connected in the attack graph $C_{min}(k \dashrightarrow l)$ will be set to infinity. Besides, the outputs of all five equations above are normalized to interval $[0, 1]$.

After getting alignment scores for candidate permutations of each technique, we will compare them with pre-defined threshold and finally select aligned subgraphs of techniques. It is noteworthy that one attack graph node can be aligned in

multiple techniques, and one technique can be found multiple time as long as each aligned subgraph have an alignment score above the threshold.

TKG construction. With the graph alignment results, we can attach the general knowledge stored in technique templates, including alternative entities and techniques, to the corresponding positions in an attack graph. Then we get the Technique Knowledge Graph (TKG) that introduces the whole attack chain in a CTI report with enhanced knowledge.

3.3.3 Initialization and Updating of Technique Templates

Both the updating and the initialization of technique templates rely on the graph alignment results. The node in the attack graph can be mapped to the node in the identified technique template with alignment results. Then we update the IoC and natural language description sets in the template node with probably new terms from the aligned attack graph node. This allows us to aggregate threat intelligence across massive CTI reports at the technique level.

The initialization process of technique templates start with a random single-technique attack graph extracted from MITRE technique examples as the initial template. Then we align the initial template with other single-technique attack graphs of the same technique. The information in aligned attack graph nodes will be merged into corresponding template node, and the unaligned nodes will be added to templates as new nodes. Finally, we get the technique template that aggregates threat intelligence and covers multiple technique

variants across multiple reports, as shown in Figure 3 and Table 3.

4 Evaluation

In this section, we focus on evaluating AttackKG’s accuracy of attack graph extraction and technique identification as a CTI report parser and its effectiveness of technique-level intelligence aggregation as a CTI knowledge collector. In particular, our evaluation aims at answering the following research questions: (RQs):

- **RQ1:** How accurate is AttackKG in extracting attack graphs (attack-related entities and dependencies) from CTI reports?
- **RQ2:** How accurate is AttackKG in identifying attack techniques in CTI reports?
- **RQ3:** How effective is AttackKG in collecting technique-level intelligence from massive CTI reports?

4.1 Evaluation Setup

To evaluate AttackKG, we collect 1,515 real-world CTI reports from diverse intelligence sources, such as Cisco Talos Intelligence Group [1], Microsoft Security Intelligence Center [14], and DARPA Transparent Computing (TC) program [4]. Moreover, we crawl 7,373 procedure examples out of 179 techniques from MITRE ATT&CK knowledge-base [11] to formulate our technique templates.

To answer RQ1 and RQ2, we further manually label the ground-truth of entities, dependencies, and techniques in eight of the collected reports: (1) *Five DARPA TC Reports*: We select five attack reports released by the DARPA TC program that cover different OS platforms (i.e., Linux, Windows, and FreeBSD), vulnerabilities (e.g., Firefox backdoor), and exploits (e.g., Firefox BITS Micro). Specifically, the attacks in the report are generated during the fifth red-team vs. blue-team adversarial engagement in May 2019 [17]. The engagement sets up an isolated network for two weeks to simulate an enterprise environment with different security-critical services, such as email and SMB servers. During the engagement, the red team carries out several APT campaigns to exfiltrate proprietary information on target systems. The descriptions of the attacker’s activities are recorded in natural language by the red-team members as the ground-truth attacks in the final reports. (2) *Three APT Campaign Reports*: To explore the performance of AttackKG in practice, we select another three public CTI reports that describe APT campaigns from three well-known threat groups, i.e., Frankenstein [5], OceanLotus (APT32) [13], and Cobalt Group [12].

4.2 Evaluation Results

4.2.1 RQ1: How accurate is AttackKG in extracting attack graphs from CTI reports?

A typical attack technique consists of multiple threat actions that are presented as a set of connected entities in an attack graph. In particular, the accurate extraction of attack graphs is an essential starting point towards automated identification of attack techniques from CTI reports. To evaluate the accuracy of AttackKG in extracting attack graphs, we adopt the aforementioned eight well-labeled CTI reports. We manually identify attack-related entities in the reports and correlate entities based on our domain knowledge of the attack workflow. It is noteworthy that in addition to natural language descriptions, DARPA TC reports also provide the graph representation of attacks, which serves as additional documentation to complement our manual labels. Detailed labeling results are available in Appendix A.

Given ground-truth entities and dependencies in the reports, we are able to compare AttackKG with the state-of-the-art open-source⁴ CTI report parser, EXTRACTOR [43], in terms of the precision, recall, and F1-score. For a fair comparison, we enable all optimizations in EXTRACTOR (e.g., Ellipsis Subject Resolution) when constructing attack graphs upon textual attack descriptions. As discussed in Section 3, an entity may correspond to multiple co-references across a CTI report. Since our goal is to identify unique entities (e.g., IOCs), we merge co-reference entities in the attack graph and integrate their dependencies with the remaining entities.

Table 5 summarizes the results of AttackKG and EXTRACTOR in capturing entities and dependencies from the selected eight CTI reports. As can be seen, compared to the baseline approach EXTRACTOR, AttackKG generally introduces more false-positive entities. This is expected as EXTRACTOR aggregates all non-IoC entities of the same type (e.g., process) into one entity, as shown in Figure 1. In other words, no matter how many false-positive entities EXTRACTOR produces, they are treated as one false extraction as long as they belong to the same type. However, this aggregation design inevitably loses structural information of attack graphs and makes follow-up technique identification almost impossible. Hence, we only compare AttackKG with EXTRACTOR in extracting attack graphs rather than identifying attack techniques. Despite lower precision caused by a higher false-positive rate, AttackKG still yields better accuracy overall (with an average F1-score improvement of 0.12) than EXTRACTOR due to a much lower false-negative rate. From Table 5, we also observe that compared to public CTI reports, AttackKG achieves better performance when extracting attack graphs from DARPA TC reports. This is reasonable as DARPA TC reports are primarily designed to record attackers’ activities, while public CTI reports systematically analyze

⁴<https://github.com/ksatvat/EXTRACTOR>

Table 5: Accuracy of attack graph extraction and technique identification in eight CTI reports. (Rows 2-9 present the count of manually-generated ground-truth and *-false_negative(+false_positive)* in extracting attack-related entities, dependencies, and techniques. Rows 10-12 present the overall Precision, Recall and F1-score.)

CTI reports	Entities			Dependencies			Techniques		
	Manual	EXTRACTOR	AttackKG	Manual	EXTRACTOR	AttackKG	Manual	TTPDrill	AttackKG
TC_Firefox DNS Drakon APT	10	-4 (+4)	-0 (+1)	9	-4 (+3)	-2 (+1)	8	-2 (+10)	-0 (+3)
TC_Firefox Drakon APT Elevate Copykatz	6	-2 (+0)	-1 (+0)	5	-2 (+0)	-2 (+0)	4	-1 (+13)	-1 (+0)
TC_Firefox BITS Micro APT	11	-6 (+0)	-1 (+4)	10	-7 (+0)	-0 (+0)	5	-1 (+14)	-2 (+2)
TC_SSH BinFmt-Elevate	6	-4 (+0)	-1 (+0)	5	-4 (+0)	-0 (+0)	5	-2 (+14)	-2 (+2)
TC_Nginx Drakon APT	15	-2 (+0)	-2 (+0)	15	-0 (+0)	-2 (+0)	6	-2 (+22)	-0 (+2)
Frankenstein Campaign	14	-3 (+1)	-0 (+2)	16	-5 (+1)	-0 (+2)	9	-1 (+18)	-1 (+1)
OceanLotus(APT32) Campaign	7	-0 (+2)	-0 (+2)	7	-0 (+1)	-1 (+0)	5	-1 (+12)	-2 (+0)
Cobalt Campaign	17	-6 (+0)	-1 (+5)	17	-4 (+0)	-1 (+4)	8	-2 (+21)	-1 (+1)
Overall Precision	1.000	0.894	0.853	1.000	0.921	0.906	1.000	0.233	0.782
Overall Recall	1.000	0.686	0.942	1.000	0.690	0.917	1.000	0.760	0.860
Overall F-1 Score	1.000	0.776	0.895	1.000	0.789	0.911	1.000	0.357	0.819

Table 6: Ablation study of different components used in technique identification.

	Techniques		
	Precision	Recall	F1-Score
w/ all component	0.782	0.860	0.819
w/o IoC information	0.833	0.600	0.698
w/o natural language text	0.690	0.800	0.741
w/o dependencies	0.667	0.480	0.558
w/o graph simplification	0.696	0.780	0.736

how an attack works. Therefore, public CTI reports tend to be longer with more technical details, which may mislead AttackKG to generate false-positive entities and dependencies.

4.2.2 RQ2: How accurate is AttackKG in identifying attack techniques in CTI reports?

To answer RQ2, we use AttackKG to identify attack techniques in the eight CTI reports and compare it with the state-of-the-art technique identifier, TTPDrill [30]. The core idea of TTPDrill is to extract threat actions from CTI reports and attribute such actions to techniques based on threat-action ontology. Specifically, it manually defines 392 threat actions for 187 attack techniques in the original paper, while such ontology knowledge base has been extended to cover 3,092 threat actions for 246 attack techniques in its latest open-source implementation⁵. Also noteworthy is that all attack techniques used by TTPDrill are derived from an old version of Mitre ATT&CK matrix. To allow for a consistent comparison, we map every technique in TTPDrill to the latest version technique via the hyperlinks provided by MITRE. For example, T1086-PowerShell⁶ in TTPDrill is updated to T1059/001-Command and Scripting Interpreter: PowerShell⁷.

We evaluate AttackKG and TTPDrill on the eight CTI re-

ports that we know the precious ground-truth techniques adopted in the attacks. The technique identification results are summarized in the last three columns in Table 5. We can observe that while both AttackKG and TTPDrill achieve reasonably low false-negative rates, TTPDrill is prone to high volumes of false-positive techniques (15.5 false positives per report on average), which is nearly three times as many as the true positives. For example, *TC_Nginx Drakon APT* report only has six true-positive techniques, but TTPDrill gives over 20 false positives. As a result, while the recall of AttackKG is only slightly higher than TTPDrill by 0.1, AttackKG significantly outperforms TTPDrill in terms of the precision and F1-score by 0.549 and 0.426, respectively. This result makes sense as TTPDrill treats threat actions extracted from CTI reports as a bag of words without considering their interactions. Accordingly, techniques under the same tactic that share partial threat actions tend to look similar to each other in TTPDrill. In contrast, AttackKG aligns techniques to attack graphs, taking into consideration the full contexts of threat actions.

Ablation Study of AttackKG. To verify the impact of each component in AttackKG towards technique identification, we perform an ablation study by considering four variants of AttackKG. In particular, we first remove part of the attributes in entities: the IoC information and natural language text termed *AttackKG_{w/o IoC information}* and *AttackKG_{w/o natural language text}*, respectively. Note that unlike the EXTRACTOR’s practice of merging entities, we only remove partial entity attributes without sacrificing the structural information of attack graphs. Moreover, we obtain another variant by filtering out dependencies in attack graphs termed *AttackKG_{w/o dependencies}*. That is, we predict attack techniques only based on entity sets. Finally, we disable the graph simplification component termed *AttackKG_{w/o graph simplification}*.

As different component combinations may affect the distribution of alignment scores, we adjust and choose identification thresholds separately for AttackKG variants in light of the optimal F1-scores. The experimental results are summarized

⁵<https://github.com/mpurba1/TTPDrill-0.3>

⁶<https://attack.mitre.org/techniques/T1086>

⁷<https://attack.mitre.org/techniques/T1059/001>

Table 7: Effectiveness of Threat Intelligence Extraction from 1,515 CTI Reports.

Top 10 Techniques	Occurrences in reports	#Unique IoCs				
		Executable	Network	Files/Directions	Registry	Vulnerability
T1071 - Command & Control	1113	12	452	371	-	12
T1059 - Command and Scripting Interpreter	1089	6	394	284	100	9
T1083 - File and Directory Discovery	1060	-	-	249	-	-
T1170 - Indicator Removal on Host	990	6	-	255	74	7
T1105 - Ingress Tool Transfer	990	-	389	261	-	-
T1003 - OS Credential Dumping	961	-	-	220	-	-
T1204 - User Execution	862	-	209	180	-	-
T1566 - Phishing	839	6	267	307	-	5
T1574 - Hijack Execution Flow	816	-	-	70	-	-
T1005 - Data from Local System	792	-	-	197	-	-
T1218 - Signed Binary Proxy Execution	664	17	-	81	37	-
All Techniques Summary	28262	495	2813	4634	384	67

in Table 6. We find that removing any component would degrade AttackKG’s overall performance, which well justifies our design choice. Especially, $AttackKG_{w/o \text{ dependencies}}$ consistently performs the worst across all evaluation metrics. It verifies the substantial influence of graph structures in technique identification.

4.2.3 RQ3: How effective is AttackKG at collecting technique-level intelligence from massive reports?

To answer RQ3, we explore the effectiveness of AttackKG in identifying techniques and IoCs entities on 1,515 CTI reports collected from different intelligence sources. It is worth mentioning that IoC entities in a CTI report are sometimes not related to any technique. We do not include such IoC entities in our statistics as they are unlikely to convey substantive information about how an attack behaves.

Table 7 shows ten techniques with the largest amount in the 1,515 reports and the number of their corresponding unique IoCs. Each report, on average, contains 18.7 techniques and 5.5 IoCs, and different techniques in most cases involve different IoCs. We observe that the most frequently used technique is the T1071-Command & Control which is related to the high popularity of the command and control tactic in the lifetime of APT attacks. In particular, a tactic explain “why” an attacker performs an action while a technique describes “how” the action is achieved. By discovering tactics to which the techniques in Table 7 belong, we find that ten techniques correspond to eight tactics (i.e., Command and Control, Execution, Discovery, Defense Evasion, Credential Access, Initial Access, Persistence, and Collection). It is not surprising to observe that the most commonly used techniques are from different tactics. In fact, this experimental result mirrors our intuitive understanding of the lifecycle (i.e., kill chain) of an attack, where a typical attack must consist of a set of unique tactics while each tactic can be achieved with different techniques.

From Table 7, we also see that the number of identified techniques is larger than that of IoCs. There are two main reasons behind this observation: (1) We only count unique IoCs. That is, redundant IoCs are only counted once; (2) Techniques are sometimes presented as interactions among non-IoC entities. For instance, “All observed attacks start with an email message, containing either a malicious attachment or a URL which leads to the first stage of the attack” introduces a phishing technique without incorporating any IoC description.

4.3 Case Study

To gain further insight, we visually demonstrate the knowledge extracted by AttackKG from CTI reports about two real-world APT attacks, namely, the Frankenstein and Cobalt campaigns. Frankenstein campaign is the APT attack on which the motivating example in Figure 1 focuses. In this subsection, we present how AttackKG parses the report in Figure 12 that describes the Cobalt campaign. The Cobalt Group is a financially motivated APT group that primarily targets financial institutions like the Government Saving Bank in Thailand and First Commercial Bank in China. This group has conducted intrusions to steal money via breaching ATM systems, card processing, payment systems, and SWIFT systems [16].

Figure 4 illustrates the attack graphs and technique knowledge graph (TKG) automatically built upon the Cobalt CTI report. In specific, Subfigure (A) shows the attack graph extracted by AttackKG with contained attack techniques, while Subfigure (B) depicts the attack graph extracted by EXTRACTOR. As can be observed, compared to EXTRACTOR, AttackKG presents much more semantic information about the Cobalt campaign by identifying non-IoC entities such as *RTF file* and *JScript backdoor*. Furthermore, by discovering techniques and technique relations, security analysts can easily summarize the attack kill chain, as shown in Subfigure (C), and quickly understand the attack workflow. We would like to point out that although AttackKG misses one true-positive tech-

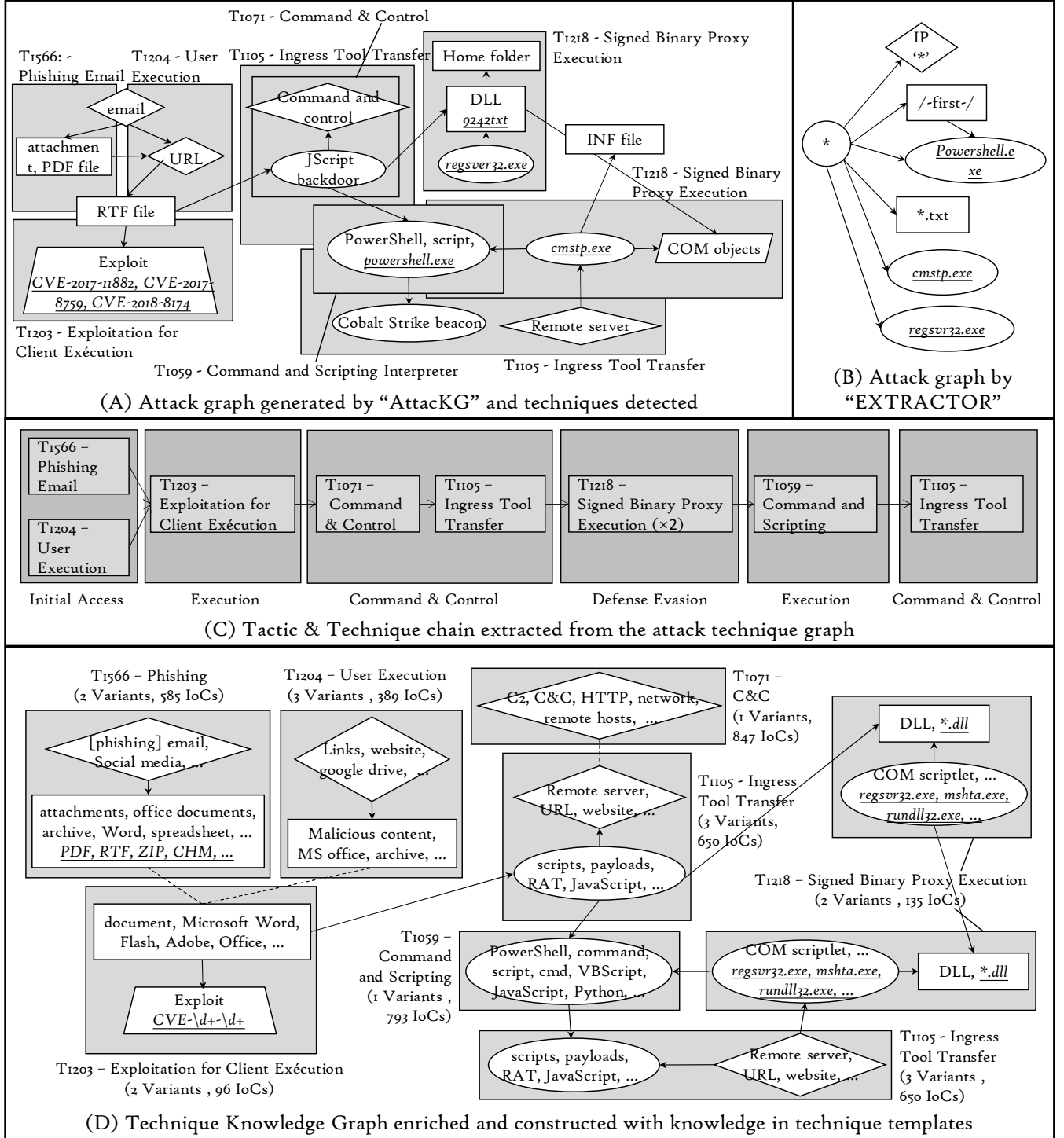


Figure 4: A case study of the Cobalt campaign. The original CTI report is presented in Figure 12. For clarity, we have omitted false-positive nodes and edges for presentation. Specifically, Subfigure (A) illustrates the attack graph extracted from the report and the technique detected by our approach. As a comparison, Subfigure (B) shows the attack graph extracted by EXTRACTOR. Subfigure (C) shows the technique-level attack chain retrieved from the report. And Subfigure (D) presents the Technique Knowledge Graph (TKG) generated for this report. As shown, we can find different variants and related IoCs for each attack technique, and these techniques are connected with the heuristics from the report.

nique (i.e., T1027-Obfuscated Files or Information) available in the report, analysts can still make sense of the overall attack without missing critical information as the primary attack workflow is preserved. AttackKG also generates a false-positive technique (i.e., T1070-Indicator Removal on Host) that indicates the attacker’s footprint cleanup. We attribute such the false positive to the fact that AttackKG does not differentiate relations for dependencies, and any file access (e.g., deleting and writing) is considered equally. As a result, the representative threat action (e.g., system file deletion) in T1070 cannot be distinguished, which causes T1070 to be commonly identified as the false-positive technique. Subfigure (D) presents the Cobalt campaign’s TKG enhanced by the technique templates derived from 7,373 procedure examples in MITRE. With such a TKG, we can learn different potential Cobalt implementations (e.g., using different IoCs) beyond the report, which directly benefits downstream security tasks such as APT attack detection and investigation.

5 Related Work

Threat Intelligence Extraction Cyber threat intelligence (CTI) plays a vital role in security warfare to keep up with the rapidly evolving landscape of cyber attacks [20, 41]. To facilitate CTI knowledge exchange and management, the security community has standardized open formats (e.g., OpenIoC [9], STIX [6], and CyBOX [3]) to describe Indicators of Compromises (IoCs). For example, OpenIoC typically describes malware samples as a list of binaries with loaded DLLs. Though structured and machine-readable, such information is insufficient to understand how an attack behaves as it lacks descriptions of interactions among IoCs. In addition to standard formats, cyber attacks are often introduced in natural language reported in technical blogs, white papers, or posts. While such CTI reports provide detailed contexts about an attack (e.g., the sequence of adversarial actions), manually extracting attack-relevant information from uninstructed texts is labor-intensive and error-prone, hindering CTI’s practice applications.

Researchers have recently started to learn knowledge contained in CTI reports automatically. Based on the observation that IoCs often share similar context terms, iACE [36] presents a graph mining technique to collect IoCs available in tens of thousands of security articles. ChainSmith [49] further makes use of neural networks to classify IoCs into different attack campaign stages (e.g., baiting and C&C). TTPDrill [30] derives threat actions from Symantec reports and maps them to attack patterns (e.g., techniques in MITRE ATT&CK [11]) pre-defined as ontology. EXTRACTOR [43] and ThreatRaptor [21] customize NLP techniques to model attacks behaviors in texts as provenance graphs. Similar to prior studies, the large body of AttackKG is to automate knowledge extraction from CTI. Nevertheless, AttackKG distinguishes from these works in the sense that it identifies TTPs and constructs a

technique knowledge graph (TKG) to summarize CTI reports. Unlike low-level provenance graphs, TKG provides a high-level visualization of multi-stage attacks using TKGs, which accelerates the attack interpretation process [25]. Although TTPDrill also aims to identify techniques in CTI, it considers each technique as independent actions, failing to reconstruct complete attack scenarios.

Threat Detection with Cyber Intelligence Recent advancements of causality analysis in system auditing [19, 31, 32, 42] have enabled security investigators to detect cyber attacks with multiple stages. However, audit logs monitor general-purpose system activities and thus lack the knowledge of high-level behaviors [48]. In most cases, analysts act as the backbone in SOCs (security operations center) to correlate various attack stages through reviewing numerous system logs [45]. Unfortunately, as the volume of audit data is typically overwhelming even after reducing noisy logs irrelevant to attacks [27, 33, 37, 38, 44, 47], it is infeasible to manually analyze cyber threats directly based on audit logs [22, 23].

CTI has proved to be valuable information in navigating audit logs and pinpointing behaviors associated with known attacks [21, 25, 28, 39, 40]. For example, RapSheet [25] matches audit logs against a knowledge base of TTPs (Tactics, Techniques, and Procedures) from MITRE. Then, it correlates TTPs in logs and constructs a TPG (tactic provenance graph) to recover *kill chains* in APT campaigns. The scope of AttackKG is different from RapSheet as RapSheet primarily adopts TTPs into audit log analysis to facilitate attack detection. In contrast, AttackKG brings the benefits of TTPs into CTI understanding to assist in extracting knowledge about malicious behaviors. Moreover, Poirot [39] formulates attack behaviors described in CTI reports as query graphs and presents a graph alignment algorithm to search for similar subgraphs from provenance graphs built upon audit logs.

Although threat detection based on CTI knowledge plays a critical role in commercial Endpoint Detection and Response (EDR) tools today [2], it commonly requires application-specific security policies as the initial inputs, which are time-consuming and labor-intensive to develop [40]. We envision that the deployment of AttackKG can alleviate this problem by providing a fully automated solution for constructing TKGs from CTI reports. In particular, as AttackKG can effectively summarize TTPs and TTP relations in an attack, it can be used as a foundation to implement any detectors that rely on TTP heuristics.

6 Conclusion

In this work, we propose a viable solution for retrieving structured threat intelligence from CTI reports. We use the notion of technique template to identify and aggregate technique-level threat intelligence across massive reports. Then we

leverage the knowledge contained in templates to enhance the attack graph extracted from a CTI report and generate the technique knowledge graph (TKG) that introduces the report with enhanced knowledge.

We implement our prototype system, AttacKG, and evaluate it with 1,515 real-world CTI reports. Our evaluation results show that AttacKG can extract attack graphs from reports accurately and aggregate technique-level threat intelligence from massive CTI reports effectively.

References

- [1] Cisco Talos Intelligence Group - Comprehensive Threat Intelligence. <https://blog.talosintelligence.com/>.
- [2] CTI in Security Operations: SANS 2018 Cyber Threat Intelligence Survey. https://www.domaintools.com/content/SANS_CTI_Survey_2018.pdf.
- [3] CybOX - Cyber Observable Expression. <https://cyboxproject.github.io/>.
- [4] DARPA Transparent Computing. <https://www.darpa.mil/program/transparent-computing>.
- [5] Frankenstein Campaign. <https://blog.talosintelligence.com/2019/06/frankenstein-campaign.html>.
- [6] Introduction to STIX. <https://oasis-open.github.io/cti-documentation/stix/intro.html>.
- [7] ioc parser. https://github.com/armbues/ioc_parser.
- [8] Levenshtein distance. https://en.wikipedia.org/wiki/Levenshtein_distance.
- [9] mandiant/OpenIOC_1.1. [https://github.com/mandiant/OpenIOC\[_\]1.1](https://github.com/mandiant/OpenIOC[_]1.1).
- [10] Microsoft says SolarWinds hackers stole source code for 3 products. <https://arstechnica.com/information-technology/2021/02/microsoft-says-solarwinds-hackers-stole-source-code-for-3-products>.
- [11] MITRE ATT&CK®. <https://attack.mitre.org/>.
- [12] Multiple Cobalt Personality Disorder. <https://blog.talosintelligence.com/2018/07/multiple-cobalt-personality-disorder.html>.
- [13] OceanLotus: Extending Cyber Espionage Operations Through Fake Websites. <https://www.volexity.com/blog/2020/11/06/oceanlotus-extending-cyber-espionage-operations-through-fake-websites>.
- [14] Security intelligence | Microsoft Security Blog. <https://www.microsoft.com/security/blog/security-intelligence/>.
- [15] spaCy. <https://spacy.io/>.
- [16] Threat Group Cards: A Threat Actor Encyclopedia. <https://apt.thaicert.or.th/cgi-bin/showcard.cgi?g=Cobalt%20Group>.
- [17] Transparent Computing Engagement 5 Data Release. <https://github.com/darpa-i2o/Transparent-Computing>.
- [18] Adam Bates, Kevin R B Butler, and Thomas Moyer. Take Only What You Need: Leveraging Mandatory Access Control Policy to Reduce Provenance Storage Costs. In *Proceedings of the 7th USENIX Conference on Theory and Practice of Provenance*, 2015.
- [19] Adam Bates, Dave Jing Tian, Kevin RB Butler, and Thomas Moyer. Trustworthy whole-system provenance for the linux kernel. In *USENIX Security Symposium*, 2015.
- [20] Peng Gao, Xiaoyuan Liu, Edward Choi, Bhavna Soman, Chinmaya Mishra, Kate Farris, and Dawn Song. A system for automated open-source threat intelligence gathering and management. In *SIGMOD*, 2021.
- [21] Peng Gao, Fei Shao, Xiaoyuan Liu, Xusheng Xiao, Zheng Qin, Fengyuan Xu, Prateek Mittal, Sanjeev R Kulkarni, and Dawn Song. Enabling Efficient Cyber Threat Hunting With Cyber Threat Intelligence. *ICDE*, 2021.
- [22] Peng Gao, Xusheng Xiao, Ding Li, Zhichun Li, Kangkook Jee, Zhenyu Wu, Chung Hwan Kim, Sanjeev R Kulkarni, and Prateek Mittal. SAQL: A stream-based query system for real-time abnormal system behavior detection. In *USENIX Security Symposium*, 2018.
- [23] Peng Gao, Xusheng Xiao, Zhichun Li, Fengyuan Xu, Sanjeev R Kulkarni, and Prateek Mittal. AIQL: Enabling efficient attack investigation from system monitoring data. In *USENIX ATC*, 2018.
- [24] Yali Gao, Xiaoyong LI, Hao PENG, Binxing Fang, and Philip Yu. HinCTI: A Cyber Threat Intelligence Modeling and Identification System Based on Heterogeneous Information Network. *IEEE Transactions on Knowledge and Data Engineering*, apr 2020.
- [25] Wajih Ul Hassan, Adam Bates, and Daniel Marino. Tactical provenance analysis for endpoint detection and response systems. *Proceedings - IEEE Symposium on Security and Privacy*, 2020-May, may 2020.

- [26] Wajih Ul Hassan, Shengjian Guo, Ding Li, Zhengzhang Chen, Kangkook Jee, Zhichun Li, and Adam Bates. NODOZE: Combatting Threat Alert Fatigue with Automated Provenance Triage. In *NDSS*, 2019.
- [27] Wajih Ul Hassan, Ding Li, Kangkook Jee, Xiao Yu, Kexuan Zou, Dawei Wang, Zhengzhang Chen, Zhichun Li, Junghwan Rhee, Jiaping Gui, et al. This is why we can't cache nice things: Lightning-fast threat hunting using suspicion-based hierarchical storage. In *ACSAC*, 2020.
- [28] Md Nahid Hossain, Sanaz Sheikhi, and R Sekar. Combating dependence explosion in forensic analysis using alternative tag propagation semantics. In *IEEE Security and Privacy*, 2020.
- [29] Nahid Hossain, Birhanu Eshete, Rigel Gjomemo, Sadegh M Milajerdi, Junao Wang, R Sekar, Scott D Stoller, and V N Venkatakrishnan. SLEUTH: Real-time Attack Scenario Reconstruction from COTS Audit Data. In *Usenix Security Symposium*, 2017.
- [30] Ghaith Husari, Ehab Al-Shaer, Mohiuddin Ahmed, Bill Chu, and Xi Niu. TTPDrill: Automatic and accurate extraction of threat actions from unstructured text of CTI Sources. In *ACM International Conference Proceeding Series*, volume Part F1325, 2017.
- [31] Samuel T King and Peter M Chen. Backtracking intrusions. In *SOSP*, 2003.
- [32] Samuel T King, Zhuoqing Morley Mao, Dominic G Lucchetti, and Peter M Chen. Enriching intrusion alerts through multi-host causality. In *NDSS*, 2005.
- [33] Kyu Hyung Lee, Xiangyu Zhang, and Dongyan Xu. Loggc: garbage collecting audit log. In *ACM CCS*, 2013.
- [34] Guo Li, Matthew Dunn, Paul Pearce, Damon McCoy, Geoffrey M Voelker, Stefan Savage, and Kirill Levchenko. Reading the Tea Leaves: A Comparative Analysis of Threat Intelligence. In *Usenix Security Symposium*, 2019.
- [35] Zhenyuan Li, Qi Alfred Chen, Runqing Yang, and Yan Chen. Threat Detection and Investigation with System-level Provenance Graphs: A Survey. *Computer & Security*, 106, 2021.
- [36] Xiaojing Liao, Kan Yuan, Xiaofeng Wang, Zhou Li, Luyi Xing, and Raheem Beyah. Acing the IOC Game: Toward Automatic Discovery and Analysis of Open-Source Cyber Threat Intelligence. In *CCS*, New York, NY, USA, 2016. ACM.
- [37] Yushan Liu, Mu Zhang, Ding Li, Kangkook Jee, Zhichun Li, Zhenyu Wu, Junghwan Rhee, and Prateek Mittal. Towards a timely causality analysis for enterprise security. In *NDSS*, 2018.
- [38] Noor Michael, Jaron Mink, Jason Liu, Sneha Gaur, Wajih Ul Hassan, and Adam Bates. On the forensic validity of approximated audit logs. In *ACSAC*, 2020.
- [39] Sadegh M. Milajerdi, Rigel Gjomemo, Birhanu Eshete, and V. N. Venkatakrishnan. Poirot: Aligning attack behavior with kernel audit records for cyber threat hunting. In *CCS*. Association for Computing Machinery, nov 2019.
- [40] Sadegh Momeni Milajerdi, Rigel Gjomemo, Birhanu Eshete, R. Sekar, and V. N. Venkatakrishnan. HOLMES: Real-time APT detection through correlation of suspicious information flows. *Proceedings - IEEE Symposium on Security and Privacy*, 2019-May, may 2019.
- [41] Dongliang Mu, Alejandro Cuevas, Limin Yang, Hang Hu, Xinyu Xing, Bing Mao, and Gang Wang. Understanding the reproducibility of crowd-reported security vulnerabilities. In *Usenix Security Symposium*, 2018.
- [42] Devin J Pohly, Stephen McLaughlin, Patrick McDaniel, and Kevin Butler. Hi-fi: collecting high-fidelity whole-system provenance. In *ACSAC*, 2012.
- [43] Kiavash Satvat, Rigel Gjomemo, and VN Venkatakrishnan. Extractor: Extracting attack behavior from threat reports. In *IEEE European Symposium on Security and Privacy*, 2021.
- [44] Yutao Tang, Ding Li, Zhichun Li, Mu Zhang, Kangkook Jee, Xusheng Xiao, Zhenyu Wu, Junghwan Rhee, Fengyuan Xu, and Qun Li. Nodemerger: template based efficient data reduction for big-data causality analysis. In *ACM CCS*, 2018.
- [45] Thijs van Ede, Hojjat Aghakhani, Noah Spahn, Riccardo Bortolameotti, Marco Cova, Andrea Continella, Maarten van Steen, Andreas Peter, Christopher Kruegel, and Giovanni Vigna. DeepCASE: Semi-Supervised Contextual Analysis of Security Events. In *IEEE Security and Privacy*, 2022.
- [46] Qi Wang, Wajih Ul Hassan, Ding Li, Kangkook Jee, Xiao Yu, Kexuan Zou, Junghwan Rhee, Zhengzhang Chen, Wei Cheng, Carl A. Gunter, and Haifeng Chen. You Are What You Do: Hunting Stealthy Malware via Data Provenance Analysis. In *NDSS*, 2020.
- [47] Zhang Xu, Zhenyu Wu, Zhichun Li, Kangkook Jee, Junghwan Rhee, Xusheng Xiao, Fengyuan Xu, Haining Wang, and Guofei Jiang. High fidelity data reduction for big data security dependency analyses. In *ACM CCS*, 2016.

- [48] Jun Zeng, Zheng Leong Chua, Yinfang Chen, Kaihang Ji, Zhenkai Liang, and Jian Mao. Watson: Abstracting behaviors from audit logs via aggregation of contextual semantics. In *NDSS*, 2021.
- [49] Ziyun Zhu and Tudor Dumitras. ChainSmith: Automatically Learning the Semantics of Malicious Campaigns by Mining Threat Intelligence Reports. In *IEEE European Symposium on Security and Privacy*, 2018.

A Manually Labeled CTI Report Samples

CTI Reports: The attack started by browsing to <http://128.55.12.167:8641/config.html>, selecting DNS, entering hostname [XX--ls8h.com](http://xx--ls8h.com), file 938527054, and clicking the Visit button. This triggered the **Firefox backdoor** to connect out via DNS to [XX--ls8h.com](http://xx--ls8h.com). **Drakon APT** was downloaded and executed and connected to 128.55.12.167:8640 for C2. The attacker escalated privileges using the new **File System Filter Driver**, which looks for processes opening specific files which don't exist and elevates them. Once SYSTEM, the attacker exfiltrated the host and network files as well as a passwd file in the home directory.

Attack Techniques: T1003 – OS Credential Dumping, T1005 – Data from Local System, T1041 – Exfiltration Over C2, T1059 – Command and Scripting Interpreter, (FP) T1070 – Indicator Removal on Host, T1105 – Ingress Tool Transfer, (FP) T1106 – Native API, T1204 – User Execution, T1218 – Signed Binary Proxy Execution, (FP) T1550 – Use Alternate Authentication Material, T1566 – Phishing

Figure 5: TC_Firefox DNS Drakon APT.

CTI Reports: First attacked ta51-pivot-2 and deployed OC2, allowing us to run our attack from within the target network. Exploited **Firefox backdoor** by again browsing to <http://128.55.12.233>. **Loader Drakon** was executed in **Firefox** memory and connected out to 128.55.12.233:8000 and 128.55.12.233:443 for C2. After the BBN reboot, **driver** was disabled, and we would now be able to use privilege escalation via our **perfmom driver**. We loaded the **copykatz module** to recon data from the system.

Attack Techniques: T1003 – OS Credential Dumping, T1189 – Drive-by-Compromise, T1071 – Command & Control, (FN) T1082 – System Information Discovery

Figure 6: TC_Firefox Drakon APT Elevate Copykatz.

CTI Reports: Benign activity ran for most of the morning while the tools were being setup for the day. The activity was modified so the hosts would open **Firefox** and browse to <http://215.237.119.171/config.html>. The simulated host then entered URL for **BITS Micro APT** as <http://68.149.51.179/ctfhost2.exe>. We used the **exploited Firefox backdoor** to initiate download of **ctfhost2.exe** via the **Background Intelligent Transfer Service (BITS)**. Our server indicated the file was successfully downloaded using the BITS protocol, and soon after **Micro APT** was executed on the target and connected out to 113.165.213.253:80 for C2. The attacker tried to elevate using a few different **drivers**, but it failed once again due to the computer having been restarted without disabling driver signature enforcement. BBN tried using **BCDedit** to permanently disable **driver** signing, but it did not seem to work during the engagement as the **drivers** failed to work unless **driver** signing was explicitly disabled during boot.

Attack Techniques: (FP) T1053 – Scheduled Task/Job, (FP) T1070 – Indicator Removal on Host, T1071 – Command & Control, T1105 – Ingress Tool Transfer, (FN) T1197 – BITS Jobs, (FN) T1189 – Drive-by-Compromise, T1218 – Signed Binary Proxy Execution.

Figure 7: TC_Firefox BITS Micro APT.

CTI Reports: Copied files via **SCP** and connected via **SSH** from the ta1-pivot-2 host. Sent files to the target included the privilege escalation **driver** load_helper and an elevate client. Connected to target using **SSH** with **stolen credentials**. Loaded the **driver**, and used it to gain root privileges. As root, exfil'd [/etc/passwd](http://etc/passwd), [/etc/shadow](http://etc/shadow), and the admin's home directory **Documents** files.

Attack Techniques: (FN) T1003 – OS Credential Dumping, T1005 – Data from Local System, (FP) T1070 – Indicator Removal on Host, T1071 – Command & Control, (FP) T1105 – Ingress Tool Transfer, T1218 – Signed Binary Proxy Execution, (FN) T1552 – Unsecured Credentials

Figure 8: TC_SSH BinFmt-Elevate.

CTI Reports: The attacker first tried to attack from an outside host, using 98.23.182.25:80 to download **Drakon APT** and 108.192.100.31:80 for C2. That failed, though, so the attacker switched to ta1-pivot-2 for the attack C2. The malformed **HTTP POST** was sent from 128.55.12.167 and resulted in C2 to 128.55.12.233:80. The attacker then repeated the same attack against ta1-cadets-1, exfil'ing [/etc/password](http://etc/password) from both hosts. The connections were both left open for later.

The CADETS hosts were both attacked in succession using the **Nginx Drakon APT** simulacrum.

For the attack against CADETS the exploits **Nginx** by simulation of **remote code** execution on the listening port of the **webserver** TCP 80. A malicious **HTTP** post is sent to 128.55.12.75:80 and 128.55.12.51:80 respectively. The callback is established to C2 and the following **commands** are sent to gather intelligence on the host environment: hostname, whoami, cat [/etc/passwd](http://etc/passwd), whoami, and hostname.

Attack Techniques: T1003 – OS Credential Dumping, T1005 – Data from Local System, T1059 – Command and Scripting Interpreter, T1068 – Exploitation for Privilege Escalation, (FP) T1070 – Indicator Removal on Host, T1071 – Command & Control, T1105 – Ingress Tool Transfer, (FP) T1550 – Use Alternate Authentication Material, T1599 – Phishing

Figure 9: TC_Nginx Drakon APT.

<p>CTI Reports: The threat actors sent the trojanized Microsoft Word documents, probably via email. Talos discovered a document named MinutesofMeeting-2May19.docx. Once the victim opens the document, it fetches a remove template from the actor-controlled website, https://dropbox[.]online:80/luncher.doc. Once the luncher.doc was downloaded, it used CVE-2017-11882, to execute code on the victim's machine. After the exploit, the file would write a series of base64-encoded PowerShell commands that acted as a stager and set up persistence by adding it to the HKCU\Software\Microsoft\Windows\CurrentVersion\Run Registry key. Once the evasion checks were complete, the threat actors used MSBuild to execute an actor-created file named "LOCALAPPDATA\Intel\instal.xml". Based on lexical analysis, we assess with high confidence that this component of the macro script was based on an open-source project called "MSBuild-inline-task." While this technique was previously documented last year, it has rarely been observed being used in operations. Talos suspects the adversary chose MSBuild because it is a signed Microsoft binary, meaning that it can bypass application whitelisting controls on the host when being used to execute arbitrary code. Once the "instal.xml" file began execution, it would deobfuscate the base64-encoded commands. This revealed a stager, or a small script designed to obtain an additional payload. While analyzing this stager, we noticed some similarities to the "Get-Data" function of the FruityC2 PowerShell agent. One notable difference is that this particular stager included functionality that allowed the stager to communicate with the command and control (C2) via an encrypted RC4 byte stream. In this sample, the threat actors' C2 server was the domain msdnf.lcloud. Once the "instal.xml" file began execution, it would deobfuscate the base64-encoded commands. This revealed a stager, or a small script designed to obtain an additional payload. While analyzing this stager, we noticed some similarities to the "Get-Data" function of the FruityC2 PowerShell agent. One notable difference is that this particular stager included functionality that allowed the stager to communicate with the command and control (C2) via an encrypted RC4 byte stream. In this sample, the threat actors' C2 server was the domain msdnf.lcloud. the C2 would return a string of characters. Once the string was RC4 decrypted, it launched a PowerShell Empire agent. The PowerShell script would attempt to enumerate the host to look for certain information. Once the aforementioned information was obtained, it was sent back to the threat actor's C2.</p>
<p>Attack Techniques: (FN) T1027 - Obfuscated Files or Information, T1041 - Exfiltration Over C2 Channel, T1059 - Command and Scripting Interpreter, (FP) T1070 - Indicator Removal on Host, T1105 - Ingress Tool Transfer, T1203 - Exploitation for Client Execution, T1204 - User Execution, T1218 - Signed Binary Proxy Execution, T1547 - Boot Autostart, T1566 - Phishing.</p>

Figure 10: Frankenstein Campaign.

<p>CTI Reports: The Adobe Flash install.rar archive that was returned from the baomoivietnam.com website contained the files Flash Adobe Install.exe and goopdate.dll. The table below provides some basic information on all three of these files. The file goopdate.dll has the hidden file attribute set and will not show in Windows Explorer on systems using default settings. This results in the user seeing only the Flash Adobe Install.exe file to execute in order to install what they believe to be an update to Flash Player. When run, it will automatically load goopdate.dll due to search order hijacking. Goopdate.dll is a highly obfuscated loader whose ultimate purpose is to load a Cobalt Strike stager into memory and then execute it. The Cobalt Strike stager will simply try to download and execute a shellcode from a remote server, in this case using the following URL: summerevent.webhop.net/QuUA</p>
<p>Attack Techniques: T1005 - Data from Local System, (FN) T1027 - Obfuscated Files or Information, T1105 - Ingress Tool Transfer, T1218 - Signed Binary Proxy Execution, (FN) T1574 - Hijack Execution Flow</p>

Figure 11: OceanLotus(APT32) Campaign.

<p>CTI Reports: All observed attacks start with an email message, containing either a malicious attachment or a URL which leads to the first stage of the attack. The text of the emails is likely taken from legitimate email, such as mailing lists that targeted organizations may be subscribed to. Below are three examples, with the first one purporting to be sent by the European Banking Federation and is using a newly registered domain for the spoofed sender email address. The attachment is a malicious PDF file that entices the user to click on a URL to download and open a weaponized RTF file containing exploits for CVE-2017-11882, CVE-2017-8570 and CVE-2018-8174. The final payload is a JavaScript backdoor also known as More_eggs that allows the attacker to control the affected system remotely. Notable applications used in these attacks are cmstp and msxml. The Microsoft Connection Manager Profile Installer (cmstp.exe) is a command-line program used to install Connection Manager service profiles. Cmstp accepts an installation information file (INF) as a parameter and installs a service profile leveraged for remote access connections. A malicious INF file can be supplied as a parameter to download and execute remote code. Cmstp may also be used to load and execute COM scriptlets (SCT files) from remote servers. Microsoft allows developers to create COM+ objects in script code stored in an XML document, a so-called scriptlet file. Although it is common to use JavaScript or VBScript, as they are available in Windows by default, a scriptlet can contain COM+ objects implemented in other languages, including Perl and Python, which would be fully functional if the respective interpreters are installed. To bypass AppLocker and launching script code within a scriptlet, the attacker includes the malicious code within an XML script tag placed within the registration tag of the scriptlet file and calls cmstp with appropriate parameters. An earlier part of the second stage is implemented as an encrypted JavaScript scriptlet which eventually drops a randomly named COM server DLL binary with a .txt filename extension, for example, q242.txt, in the user's home folder and registers the server using the regsvr32.exe utility. The dropper contains an encrypted data blob that is decrypted and written to the disk. The dropper then launches the next stage of the attack by starting PowerShell, msxml or cmstp.exe as described above. The PowerShell chain is launched from an obfuscated JavaScript scriptlet previously downloaded from the command and control (C2) server and launched using cmstp.exe. The first PowerShell stage is a simple downloader that downloads the next PowerShell stage and launches a child instance of powershell.exe using the downloaded, randomly named script as the argument. The downloaded PowerShell script code is obfuscated in several layers before the last layer is reached. The last layer loads shellcode into memory and creates a thread within the PowerShell interpreter process space. On the PowerShell side of the infection chain, the downloaded final payload is a Cobalt Strike beacon, which provides the attacker with rich backdoor functionality.</p>
<p>Attack Techniques: (FN) T1027 - Obfuscated Files or Information, T1059 - Command and Scripting Interpreter, (FP) T1070 - Indicator Removal on Host, T1071 - Command & Control, T1105 - Ingress Tool Transfer, T1203 - Exploitation for Client Execution, T1204 - User Execution, T1218 - Signed Binary Proxy Execution, T1566 - Phishing</p>

Figure 12: Cobalt Campaign.